# CARNEGIE INSTITUTE OF TECHNOLOGY

PITTSBURGH 13, PENNSYLVANIA

## ON THE CORROSION OF SINGLE CRYSTALS, BICRYSTALS AND POLYCRYSTALS OF AN AUSTENITIC STAINLESS STEEL IN BOILING NITRIC ACID

23 February 1962

CONTRACT Nonr 760 (14) NR 036-029



Metallurgy Branch

OFFICE OF NAVAL RESEARCH

Washington 25, D. C.

# ON THE CORROSION OF SINGLE CRYSTALS, BICRYSTALS AND POLYCRYSTALS OF AN AUSTENITIC STAINLESS STEEL IN BOILING NITRIC ACID

by

R. D. Leggett* and H. W. Paxton**

---

* Formerly Allegheny Ludlum Fellow, Carnegie Institute of Technology. Present address: General Electric Company, Richland, Washington. This paper is a portion of a thesis submitted to Carnegie Institute of Technology in partial fulfillment of the requirements for the degree of Doctor of Philosophy.

** Firth Sterling Professor of Metallurgy, Carnegie Institute of Technology, Pittsburgh 13, Pennsylvania.

## ABSTRACT

Single crystals, bicrystals and polycrystals of 20%Cr-20%Ni austenitic stainless steel were corroded in boiling nitric acid. The weight loss was independent of crystallographic orientation, grain size, and heat treatment. Metallographic observations showed no correlation between weight loss and microstructure. Adding 5 g./liter of $Cr^{+6}$, which is known to accelerate rates by one to two orders of magnitude, did not change the above conclusions. No significant change in the corrosion rates and morphologies occurred for single and bicrystals, even for those of high carbon (0.06%) and high nitrogen (0.24%) content, after ageing under conditions which normally produce marked sensitization in polycrystalline samples.

# I. INTRODUCTION

In general, austenitic stainless steels provide a most useful structural material even under severe corrosive conditions. However, it is an unfortunate characteristic of this class of materials that they fail on occasion in extremely localized areas, e.g., pitting, intergranular attack, and stress corrosion. While some of the more obvious conditions leading to these failures have been elucidated, the fact that they still occur with embarrassing frequency indicates clearly the imperfect state of our knowledge.

In polycrystalline material, it is difficult to study how corrosion rate (either as a macroscopic value or in microscopic areas) is influenced by such factors as crystallography and structural imperfections. The present study was performed in an attempt to correlate conventional weight loss measurements with observations of the surface of stainless steel single crystals and bicrystals of known orientation with the ultimate aim of seeing if this helped the understanding of the detailed mechanisms of corrosion.

The possible permutations of material, heat treatment and corrosion medium are too many to allow more than a limited survey to see how useful the technique might be. Accordingly, the variables selected were heat treatment, amount and type of interstitial solute and the crystallography of metal-liquid and metal-metal interfaces. Even with this limitation, the results obtained do not warrant a detailed listing of all the experiments performed. What follows is a selection of what the authors feel to be relevant information.

## II. EXPERIMENTAL PROCEDURE

### Materials

The bulk of the observations of this study were made on stainless steels whose compositions were so adjusted that they remained austenitic from room temperature to the melting point. This choice was made for reasons of experimental convenience, i.e., to eliminate the formation of high temperature delta ferrite during the growth of single crystals and bicrystals. Two high purity vacuum melted heats of nominal 20%Cr-20%Ni-60%Fe were kindly prepared for this investigation by Dr. A. J. Lena of the Allegheny Ludlum Research Laboratory in Brackenridge, Pennsylvania. Table I shows the analysis of these ingots together with that of a commercial type 304, which was also studied. No large differences in corrosion rate or behavior were noted between a few check tests on this Type 304 and those on the 20-20 material, but care should be taken in applying conclusions reached here to commercial compositions.

TABLE I

Analysis of the Starting Materials (wt. percent)

| Heat Number | Cr | Ni | C | N | Mn | P | S | Si |
|---|---|---|---|---|---|---|---|---|
| AL-1 | 18.05 | 19.27 | 0.0016 | 0.007 | <0.01 | 0.008 | 0.018 | <0.01 |
| AL-2 | 19.97 | 19.66 | 0.0064 | 0.0086 | <0.01 | 0.004 | 0.012 | <0.01 |
| 304 | 18.55 | 8.87 | 0.070 | 0.033 | 1.48 | 0.025 | 0.019 | 0.48 |

Heat number AL-1 was supplied in the form of 1/4" thick, hot-forged plate while heat number AL-2 was supplied in the form of a 3/4" square, hot-rolled bar.

Except for sulphur, the impurity level is much lower in both AL-1 and AL-2 than for the Type 304 stainless steel. Special care was taken, in the preparation of these alloys (with certain intentional exceptions described later),

to keep the carbon and nitrogen as low as possible due to the reported[1-13] deleterious effect of these elements on the corrosion behavior of austenitic stainless steel, particularly with regard to intergranular attack.

Preparation of Crystals

The details of the techniques developed in this study of growing single crystals and bicrystals of austenitic stainless steel have already been reported.[14] Both "strain-anneal" and "growth-from-the-melt" techniques were successful but, due to the ease of obtaining specimens for corrosion testing purposes, the latter method was most frequently employed. Basically, the process involved heating a block of alloy contained in a 15 cc recrystallized alumina boat to about 50°C above its melting point in a horizontal "globar" tube furnace and allowing it to solidify by removing the tube from the furnace at the rate of about 2-1/2" per hour.

Each ingot studied had the front tip and back tip analyzed for Cr, Ni, C and N. Typical analyses of crystals discussed in this paper are summarized in Table II. Surprisingly little segregation occurred in spite of the high alloy content of this material. Included in Table II are the analyses for two "high nitrogen" ingots and one "high carbon" ingot. Nitrogen was introduced by allowing nitrogen to flow over the molten alloy for a few minutes and then sealing off the system. Carbon was added in the form of crushed, spectroscopic graphite rod which was placed in grooves on the top of the charge. The alloy was maintained molten overnight to allow carbon diffusion to occur and then solidified in the normal manner. The high carbon ingot did exhibit some segregation with respect to the carbon content.

**TABLE II**

Analyses from the Extremes of Ingots Prepared by Directional Solidification

| | Cr | Ni | C | N | REMARKS |
|---|---|---|---|---|---|
| As Received AL-2 | 19.97 | 19.66 | 0.006 | 0.0086 | |
| L-5 Front | 19.98 | 19.89 | 0.0028 | 0.010 | grown in flowing |
| Back | 20.16 | 20.02 | 0.0030 | 0.010 | argon atmosphere |
| L-15 Front | 19.93 | 19.65 | 0.012 | 0.21 | nitrogen added and then grown |
| Back | 20.20 | 19.61 | 0.014 | 0.24 | in flowing argon atmosphere |
| L-21 Front | 19.59 | 19.40 | 0.034 | 0.016 | crushed spectroscopic graphite |
| Back | 21.20 | 19.75 | 0.062 | 0.022 | placed in grooves in charge - molten overnight, then grown in flowing argon |

Specimen Preparation

After establishing that an ingot either consisted of a single crystal or contained crystals of an appropriate size, the ingot was usually homogenized at 1300°C (which also dissolved any δ ferrite) for about 100 hours and then slowly cooled. The orientation of the crystals was determined by a back-reflection Laue technique. Thin slices of the desired orientation were then prepared by carefully cutting the crystals with a high-speed, fine abrasive, 1/32" thick, cut-off wheel. After cutting, the slices were abraded and heavily electropolished in a solution of seven parts of perchloric acid (65%) and ten parts of glacial acetic acid. The crystallographic orientation of the slices was rechecked by back reflection Laue and the specimens were then usually subjected to various heat treatments.

The heat treating was done in either purified inert gas (argon or helium) or purified hydrogen in tube furnaces controlled to $\pm$ 20°C at the highest temperatures and $\pm$ 5°C at lower temperatures. Slow to moderately rapid cooling could be accomplished without exposure to air but the quenching arrangement employed in this study necessitated a brief air exposure during the transfer from the furnace to the water. Thus, specimens that were quenched had a visible oxide film while those cooled in some other fashion usually retained the original bright surface.

Specimens were abraded once more after heat treatment and electropolished to remove all scratches. The amount of metal removed was enough to remove any possible decarburized layer. After alternate washings in water and alcohol, the specimens were dried in a blast of warm air and carefully examined under a light microscope. If the specimen was determined to be uniformly polished and free from scratches or stains, it

was immediately weighed and placed in the corrosive medium. The macroscopic surface area was determined just prior to the final polish by standard measuring techniques.

Corrosion Testing

Initially, pure boiling 65% nitric acid was used as the corrosive medium. However, the times for appreciable weight loss and microstructural changes proved to be so long that acceleration was necessary. This was accomplished by adding 9.65 g of $CrO_3$ to 1000cc of 65 $^{w}/_{o}$ nitric acid giving 5g/litre of $Cr^{6+}$.(37) It was established that this addition gave corrosion rate increases of two orders of magnitude without apparent change in surface morphology. The bulk of the tests were accordingly run in this solution and will be referred to, for convenience, as having been in "impure acid". This solution will attack grain boundaries which are not sensitized, and some caution in interpretation is thus necessary. Streicher(15) has discussed the mechanism of acceleration by the hexavalent chromium, and feels that the effect is not limited to a single process such as cathodic depolarization. The flasks and condensers described in the standard ASTM Huey test (A262-527) were used to contain the boiling acid. Each flask was heated by an individually controlled hot plate. The specimens themselves were placed either in perforated teflon baskets held in a glass cradle or in a glass basket* containing numerous holes for solution circulation. Care was taken to introduce and remove the specimens while the corrosion solution was boiling vigorously. The time of test was

* These were obtained through the courtesy of the Engineering Research Laboratory of E. I. DuPont de Nemours and Co., Inc.

carefully recorded and, in general, varied from one specimen to another and from solution to solution.

Upon removal from the corrosion solution, samples were immediately washed in hot water, rinsed with alcohol, and dried in a blast of warm air. They were then weighed and the weight loss per unit area determined. The nature and extent of the surface attack was evaluated by metallographic examination. The specimen was then corrosion tested for another period of time and this procedure repeated. Testing continued until no additional information could be obtained from the observations

## III. RESULTS AND DISCUSSION

### Crystallography

Specimens were examined as thin discs in order to obtain a preponderance of one macroscopic crystal face exposed to corrosion. Weight loss measurements in "pure" acid are shown in Table III. It will be observed that no significant difference in rate of corrosion existed between the two crystals of widely different orientation, or between these and the polycrystalline sample.

TABLE III

Corrosion Rates* of Thin Randomly Oriented Austenitic Stainless Steel Single Crystals in Pure Boiling 65 W/o Nitric Acid

| Sample No. | 0-48 Hours | 48-96 Hours | 96-144 Hours | 144-192 Hours | 192-240 Hours |
|---|---|---|---|---|---|
| W-4-A | 0.18 | 0.22 | 0.26 | 0.13 | 0.29 |
| W-4-B | 0.35 | 0.17 | 0.40 | 0.31 | 0.29 |
| Polycrystal | 0.28 | 0.24 | 0.24 | 0.28 | 0.35 |

*Reported rates are mils per month calculated for each period. The numbers may be divided by 35.9 to obtain $mg/cm^2/hour$.

As a more extensive survey, the effects of exposing (100), (110) and (111) crystal faces to "impure" acid following a wide variety of heat treatments are shown in Table IV. Table V gives the effect of superposing on prior heat treatments a standard anneal for 25 hours at 650°C. Again, in neither set of experiments was a significant effect noted on corrosion rate.

As a qualitative check of this observation a well-annealed electropolished spherical single crystal 3/4" in diameter was corroded for short

## TABLE IV

Corrosion Rates of Annealed Single Crystals of Fe-20%Cr-20%Ni in Boiling 65 w/o Nitric Acid Containing 5 g/ℓ $Cr^{+6}$

| Specimen Number | Crystal Face Exposed | Heat Treatment | Weight Loss mg/cm² | | | | |
|---|---|---|---|---|---|---|---|
| | | | 1/2* | 1 | 2 | 3 | 4 |
| L-5-1 | | As grown | 1.0 | 2.5 | --- | --- | --- |
| L-6-1 | | " " | 1.0 | 2.4 | --- | --- | --- |
| L-5-4 | 100 | " " + 1150°C-19 hr-W.Q. | --- | 1.9 | --- | --- | --- |
| L-9-7 | 110 | " " " | --- | 2.1 | --- | --- | --- |
| L-8-5 | 111 | " " " | --- | 2.0 | --- | --- | --- |
| L-5-2 | | " " + 1000°C-1 hr-W.Q. | 1.1 | 1.9 | 4.8 | --- | --- |
| L-6-2 | | " " " | 1.0 | 2.1 | 4.6 | --- | --- |
| L-8-1 | 111 | " " " | --- | 2.1 | 4.6 | --- | --- |
| L-9-3 | 111 | " " " | --- | 2.0 | 4.4 | --- | --- |
| L-11-4 | 100 | 1300°C - 72 hr - F.C. | --- | 1.9 | --- | --- | 10.1 |
| L-5-3 | 100 | As L-11-4 + 1000°C - 1 hr - W.Q. | --- | 1.6 | --- | 5.7 | --- |
| L-9-9 | 110 | " " | --- | 2.1 | --- | 7.1 | --- |
| L-9-6 | 111 and 110 | " " | --- | 2.3 | --- | 6.7 | --- |
| L-8-2 | 111 | " " | --- | 2.0 | --- | 7.2 | --- |
| L-6-6 | 111 | " " | --- | 1.8 | --- | 7.1 | --- |
| L-11-1 | 100 | " " | --- | 2.1 | --- | --- | 9.1 |
| L-11-2 | 100 | " + 900°C - 24 hr - W.Q. | --- | 1.7 | 4.8 | --- | 9.3 |
| L-9-6 | 111 and 110 | " " | --- | 2.3 | --- | --- | --- |
| L-11-3 | 100 | " + 1100°C - 24 hr - W.Q. | --- | 1.7 | 4.5 | --- | 8.1 |
| L-9-9 | 110 | " + 1100°C - 24 hr - S.C. | --- | 2.0 | --- | --- | --- |
| L-6-3 | 111 | As grown + 1100°C - 5 min - W.Q. | --- | 1.3 | 3.6 | --- | 8.2 |
| L-6-4 | 111 | " + 1100°C - 1 hr - W.Q. | --- | 1.8 | 4.0 | --- | 8.5 |
| L-6-5 | 111 | " + 1100°C - 6 hr - W.Q. | --- | --- | 4.2 | --- | 9.4 |

* Hours in test
W.Q. - Water Quenched
F.C. - Furnace Cooled
S.C. - Slowly Cooled - Done by moving samples to cold portion of horizontal furnace.

## TABLE V

Corrosion Rates of Single Crystals of Fe-20%Cr-20%Ni in Boiling 65 w/o Nitric Acid Containing 5 g/ℓ $Cr^{+6}$ After Annealing at 650°C for 25 hours

| Specimen Number | Crystal Face Exposed | Prior Thermal History | Weight Loss Mg/cm² | | | |
|---|---|---|---|---|---|---|
| | | | 1* | 2 | 4 | 10 |
| L-5-5 | 100 | As Grown | 0.3 | 2.9 | 7.8 | 23.5 |
| L-6-7 | 111 | As Grown | 1.4 | 4.4 | 10.0 | 27.6 |
| L-8-3 | 111 | As Grown | 1.4 | 4.0 | 8.9 | 25.8 |
| L-9-4 | 111 | As Grown | 0.9 | 3.5 | 8.6 | 27.1 |
| L-11-5 | 100 | 1300°C-72 hrs.-F.C. | 1.0 | 3.8 | 9.4 | 25.7 |
| L-5-3 | 100 | 1300°C-72 hrs.-F.C.+1000°C-1 hr.-W.Q. | 0.5 | 2.6 | 6.4 | 18.3 |
| L-6-6 | 111 | 1300°C-72 hrs.-F.C.+1000°C-1 hr.-W.Q. | 1.6 | 3.8 | 8.0 | 21.5 |
| L-8-2 | 111 | 1300°C-72 hrs.-F.C.+1000°C-1 hr.-W.Q. | 1.4 | 3.7 | 7.8 | 21.3 |
| L-9-6 | 111 and 110 | As L-5-3 + 900°C-24 hrs.-W.Q. | 0.9 | 2.8 | 6.4 | 18.2 |
| L-9-9 | 110 | As L-5-3 + 1100°C-24 hrs.-S.C. | 1.0 | 2.8 | 6.2 | ---- |

* Hours in test

and long periods of time in pure boiling 65 $^{w}/_{o}$ nitric acid. No evidence of enhanced or retarded corrosion-rates at certain orientations was observed. In unpublished work, Fiore[16] has made a similar observation from 200 to 700°C in oxygen pressures of 0.4 to 0.75 atm on oxidation of monocrystalline spheres in stainless steel. Basinska et al[17] showed that the rate of formation of an anodised film on aluminum was not altered in any of the orientations used in their experiments. These results are in sharp contrast to the results obtained by Gwathmey and his co-workers[19-23], Lustman[24], Mehl[25] and Mehl and McCandless[26-27] on the oxidation rates in air of oriented Cu and Fe.

In addition, Dobrian[18] has shown that straining single crystals 2 or 5% in tension prior to a corrosion test in impure acid has no effect, and that, in spite of slip lines readily visible on the surface, the pattern of attack was unchanged.

On the other hand, a reducing corrodent ($HCl-H_2O-H_2O_2$) caused the $\langle 100 \rangle$ planes to be clearly developed very rapidly. This observation is in accord with many current views of transport of atoms to or from a clean solid surface which assume that the rate will depend on the density and efficiency of surface imperfections such as ledges and kinks[28-30].

Morphological Features

In view of the closely similar macroscopic corrosion rates, one might expect little difference in appearance between corroded surfaces. In fact, substantial differences were noted after various heat-treatments but apparently these did not contribute significantly to weight loss. This is perhaps the most important observation reported here.

A typical structure is shown in Figure 1. Pits form both along sub-boundaries and within the sub-grains with a tendency to avoid the region next to the sub-boundary. Lineal analysis to determine size and number of pits, and assumption of various reasonable shapes showed that these pits contributed at most a few percent of the observed weight loss. The much larger black pits result from the solution of inclusions, identifiable in the unetched state as primarily $Cr_3O_4$.[31] These pits provide also only a small contribution to the total corrosion. It appears that the bulk of matter transported passes through the visible oxide film leaving traces, if any, on a scale finer than that observable here.

In order to obtain a proper perspective on the attack, it must be remembered that $1 mg/cm^2$ dissolved corresponds to slightly more than 1μ of metal removed. Since the "oxide films",* as judged from the straw color developed after several hours in impure acid, are a few hundred Å thick, it is apparent that continuous formation and solution of oxide is taking place during a test with the oxide film at any one time being a very small fraction of the volume of metal removed.

It is also possible that a thin protective oxide, whose thickness is essentially constant with time, or which breaks down and heals at a constant frequency,[15] is present under the visible oxide, and that transport through this film is rate determining. Experimental proof of this would be quite difficult.

*The composition of the corrosion film was not determined. Rhodin[36] has suggested that thick films (a few hundred Å) consist of spinels; the degree of hydration is also not known. For simplicity, we use the term "oxide film" with these reservations.

In spite of the thickening of the oxide during test, the rate of weight loss remains substantially linear and varies little from specimen to specimen. To confirm this rather surprising observation, a qualitative experiment was performed. The corrosion rate of freshly electropolished crystals was compared with that of crystals oxidized at 625°C in air to give a light straw (L 22-2) and a dark straw (L 22-1) oxide film. In spite of these pronounced differences between the initial surface, the corrosion rates are indistinguishable even in the very earliest stage after 1/2 hour in the corrosive solution. (Figure 2). This must mean that the rate limiting step is not mass transport through the visible film, and that these thick films have little protective value.

An interesting observation was made on the pitting patterns. An initial pattern was set up on the electropolished sample, and subsequent corrosion accentuated this pattern without changing the distribution of the pits or their number. Furthermore, even after several microns of metal had been removed, the pits retained the same relative positions indicating they were growing approximately perpendicular to the surface. It seems unlikely that emergent dislocations would remain as straight for such distance. Although, as will be seen later, the number of pits decreased with increasing annealing temperature, the rate of weight loss did not change. Accordingly, a model (assuming the pits are caused by dislocations) invoking anion diffusion along the oxide-metal interface followed by rapid pipe diffusion through the oxide is not tenable since the mean diffusion distance to the nearest dislocation varies.

Bicrystal Specimens

The morphological features of each grain of a bicrystal were similar to those in single crystals. The grain boundary itself was attacked in a manner described below, depending on mis-orientation and heat treatment. On each side of the grain boundary essentially no pitting attack took place in a region whose width depended on annealing temperature and mis-orientation. As will be seen in Figure 3, the width of this unattacked zone for a large-angle boundary varies from 1μ or less after a 650°C anneal to about 10μ at 1100°C. The width of this unattacked zone also became noticeably smaller as the misorientation between grains decreased. (See Figure 4 for example).

That this zone was in some sense truly different from the matrix, and not due to electrochemical protection, was demonstrated by examination of a bi-crystal with the pole of the boundary making an angle of some 15° with the surface normal. The unattacked zone was widened geometrically as expected after short exposures. Further corrosion of this specimen led to the conclusion that the nucleation of pits in this zone is difficult, but that once a pit is nucleated, it will continue to grow into the specimen while enlarging slightly laterally. This leads in this specimen ultimately to the disappearance of the unattacked zone since after some time all areas on it have had a pit nucleated above them either in the grain boundary or in the unaffected material as shown schematically in Figure 5, and as micrographs in Figure 6.

In a specimen where the grain boundary is essentially normal to the surface, the unattacked zone persists at least up to the limit of testing time used here.

The density of pits was influenced by annealing temperature. After an 1100°C anneal, the pit density was low. As annealing temperature decreased, the pit density increased and a tendency towards crystallographic alignment resulted. At first sight, it might seem that this is due to precipitation on slip planes produced accidentally during handling. However, crystals deliberately strained at room temperature and subsequently aged showed no such patterns; if accidental deformation was produced at elevated temperatures, there is no simple way of reproducing it in a convincing fashion.

The severity of boundary attack for a given large misorientation between grains was a minimum after a 900°C anneal, often more marked than that shown in Figure 3. This attack was reproducible, and almost a "state function" in that annealing at, say, 1100°C followed by a 900°C treatment produced the type of attack typical of a single 900°C treatment.

The boundary attack was investigated by sectioning and multiple beam interferometry to follow the depth of attack. The attack was at all temperatures of annealing, in general not deeper than 3 times the surface width of attack, except in some experiments on polycrystals, discussed later. The difference in level between two adjacent grains after test was at most of order 2000 Å, i.e., each grain was dissolving at essentially the same rate as its neighbor of different orientation.

As might be expected from the results cited above, the observed rates of weight loss were insensitive to change in original area of each grain present in a bicrystal or to the relative orientation of each grain.

The attack at a grain boundary was minimised when two grains had very similar lattice orientations, i.e. when the grain boundary energy is low. Variations in the spacial plane of the boundary itself caused second order effects in these low energy boundaries and, on occasion, no attack at all occurred.

Polycrystalline Specimens

Several workers[15,32,33,37,38] have observed that polycrystalline commercial austenitic steel is attacked rapidly, particularly at grain boundaries in 65% nitric acid especially if $Cr^{6+}$ is present. This is true whether or not the steel has carbides precipitated at the boundaries. In experiments carried out on material AL-2 (which contains much less than 0.01%C and N-- see Table 1) in the as received condition (hot rolled), and also after annealing at 900°C or 1100°C for 24 hours, this observation was confirmed. (Figure 7).

In the sample annealed at 900°C after hot rolling, "ghost" boundaries are clearly visible, each with its own pit-free zone. The extent and type of attack at these ghost boundaries is quite different from that at existing grain boundaries, and must indicate a persistent type of segregation and/or a stable dislocation network.

This behaviour is not in accord with the observations on the much larger grained examples discussed earlier in that the grain-boundary attack in polycrystalline material is heavy even after a 900°C anneal and the pitting is much less. If this grain boundary attack could be controlled as it was in bi-crystals, the problem of grain dropping which leads to large effective corrosion rates would be minimised greatly. It proved possible to do this by recrystallizing a single crystal of 20 Cr-20

Ni (which had been cold rolled 65%) at 1100°C for 24 hours, slow cooling, and annealing at 900°C for 24 hours, followed by a water quench. This specimen gave a linear corrosion rate with no grain dropping (Figure 8).

A detailed series of experiments is planned to check on this most interesting observation, since it appears that it may be possible to control this particular form of grain boundary corrosion by heat treatment. It should be noted that this treatment should probably not be confused with that given at about 900°C to precipitate carbides in such a form that the amount of subsequent intergranular corrosion is minimised. The accepted solubility for C & N is 19Cr-10Ni apparently at 900°C is not less than 0.01%[15,39] and is not known for 20Cr-20Ni.

Once again the overall corrosion rates in these experiments agreed within experimental error with those on single crystals and bicrystals (except when grain dropping occurred) and the surface morphologies must contribute little to observed weight losses.

The Influence of Carbon and Nitrogen

The high nitrogen (0.24%N) and high carbon (0-06%) ingots were prepared to examine the influence of these elements on the corrosion behaviour of single and bi-crystals. In polycrystalline material, it is of course well established that precipitation of carbides causes accelerated attack on grain boundaries in certain media of which nitric acid is one[1-13,15,34,35,38]. The $Cr^{6+}$ used in the tests should accentuate any tendency to preferential grain boundary attack.

The crystals were annealed at various temperatures from 650°C to 1150°C (inclusive) and water quenched. Measurements of microstructure and macroscopic weight loss were made as usual. The rates of corrosion are shown in Figure 9 along with those for some of the very low carbon

and nitrogen crystals. No significant differences were present.

The morphology, even after ageing the 0.06%C specimens at 650°C, which normally causes the most severe accelerated grain boundary attack, was also not significantly different from that present in low-carbon specimens. However, polycrystalline samples of L-21(0.06 $^{w}/_{o}$C) prepared by cold rolling single crystals, recrystallizing at 1050°C, and ageing at 650°C showed the marked grain boundary attack characteristic of sensitized samples, and grain dropping occurred early in the test. In the high nitrogen bicrystals, after annealing at 800°C, a clearly visible precipitate was present (Figure 10) but apparently caused no unusual effects.

A few experiments in boiling acid copper sulphate gave similar results in that no especially marked grain boundary attack was observed on high carbon or high nitrogen bicrystals.

## IV. GENERAL OBSERVATIONS

The major observation of this work is that the rate of general corrosion of a 20%Cr-20%Ni stainless steel in boiling 65% nitric acid, or in this solution to which 5g/litre of $Cr^{6+}$ has been added, is essentially insensitive to orientation, heat treatment, and substantial variation in carbon and nitrogen content. The addition of $Cr^{6+}$ increases general and grain boundary corrosion rates enormously, as it is known to do for polycrystalline commercial stainless steel (e.g. Types 304 and 316 which contain less nickel than the specimens used here).

Although it is not possible to compare exhaustively the results obtained here with those on commercial materials, some observations seem appropriate.

The fact that 20%Ni was used instead of 8-12% does not appear to make much difference in corrosion behaviour. Comparison of the results for single crystal and polycrystalline material (Table III) with typical results[15-38] for well annealed Type 304 in boiling 65% nitric acid show that the rates are somewhat lower for 20%Cr-20%Ni (0.3 mils per month versus about 0.5-0.6 mils per month). That the low carbon content is not responsible directly is shown in Figure 9, where the interstitial content varies widely but corrosion rates (for comparable heat treatments) in impure nitric acid do not. The microstructure after corrosion is also very similar. It seems plausible that annealed polycrystalline 20%Cr-20%Ni material containing 0.03-0.08%C would behave quite similarly to annealed Type 304 in these solutions.

The insensitivity of attack to orientation of the crystal faces exposed means that general corrosion cannot easily be controlled by pro-

ducing marked preferred orientation. However it might be feasible to reduce corrosion in solutions producing primarily grain boundary attack by use of a strong preferred orientation, or by attempting to produce the structure shown in Figure 8 by suitable heat treatments.

It was not possible to arrive at a satisfactory detailed picture of the mechanism of solution in the solutions used. The large variations in morphologies must be a secondary effect, and if these are related to dislocation-assisted solution (which is by no means certain), do not lead to a substantial contribution to weight loss. The most likely rationalization appears to be the formation and dissolution of an oxide film at equal rates leading to a constant rate of weight loss. The visible oxide films which appear in time in nitric acid, or can be obtained by air oxidation prior to corrosion testing, are probably porous and offer little protection. Direct and convincing observation of a protective film would appear to be very difficult.

It appears also that the mechanism of attack at grain boundaries, which was already known to be sensitive to precipitates and orientation difference, is even more complicated. This work has demonstrated that annealing at various temperatures prior to corrosion testing, even when no precipitation is predicted from the phase diagram, can cause a variation in intensity of attack. It seems plausible that this is related to the detailed boundary structure and the amount of segregation. Thin film electron microscopy might be helpful in improving our understanding here; further speculation does not seem warranted.

## V. CONCLUSIONS

1. The overall rate of dissolution of large crystal faces of Fe-20%Cr-20%Ni containing $<$0.01%C and N in boiling 65 w/o nitric acid with and without an addition of 5g/litre of $Cr^{6+}$ is insensitive to orientation and to the presence of grain boundaries. Addition of the $Cr^{6+}$ speeds up the rate of attack by a factor of a few hundred.
2. The morphology of attack is a complex combination of pitting and grain boundary attack dependent on thermal history and grain misorientation, but these effects are not reflected in the overall corrosion rate unless grain dropping occurs. $Cr^{6+}$ additions produce similar morphologies to those from the pure nitric acid, except that on occasion the grain boundary attack is more severe.
3. The presence of interstitial elements (C from 0.002% to 0.06% and N from 0.01% to 0.24%) in solution or as precipitates does not influence the overall rate of attack in very coarse grained specimens. Preferential grain boundary attack leading to grain dropping is observed in polycrystalline fine grained specimens of these compositions following sensitization at 650°C.
4. Some protection was observed in low carbon and nitrogen material by heat treatments which are believed not to cause precipitation of carbides or nitrides. This is in contrast to the normal stabilization heat treatment for normal carbon content at 900°C which results in precipitates in a form which is innocuous during subsequent corrosion attack.

5. Because the corrosion at a low-angle boundary is not as pronounced as at normal random boundaries, it may be possible to produce steels with greater resistance to grain boundary attack by developing strong textures.

## VI. ACKNOWLEDGMENTS

This work was supported financially by the Office of Naval Research and the Allegheny Ludlum Steel Corporation. A. J. Lena and R. C. Hall supplied materials. Valuable discussions were held with many of the authors' colleagues and with M. A. Streicher and D. Warren of E. I. Dupont de Nemours and Co., Inc. N. A. Cooper was most helpful with many of the experimental tedia.

## BIBLIOGRAPHY


1. Aborn, R. H., and Bain, E. C., "Nature of the Nickel-Chromium Rustless Steels," Trans. Am. Soc. Steel Treating, 18, 837 (1930).

2. Strauss, B., Schottky, H., and Hinnuber, J., "Carbide Formation on Annealing Stainless, Nonmagnetic, Cr-Ni Steels," Z. Anorg. allgem. chem. 188, 309 (1930).

3. Miller, J. L., "An Investigation of Certain Corrosion Resistant Steels," Iron Steel Inst. Carnegie School, Mem., 21, 111 (1932).

4. Newell, H., "Influence of Grain Size on the Properties and Corrosion Resistance of the 18-8 Iron-Chromium-Nickel Alloy, for Elevated Temperature Service," Trans. Am. Soc. Steel Treating, 19, 673 (1932).

5. Bain, E. C., Aborn, R. H., and Rutherford, J. J., "The Nature and Prevention of Intergranular Corrosion in Austenitic Stainless Steel," Trans. Am. Soc. Steel Treating, 21, 481 (1933).

6. Rollason, E. C., "Intergranular Corrosion of 18/8 Austenitic Stainless Steels," J. Iron Steel Inst. 127, 391 (1933).

7. Mahla, E. M., and Nielsen, N. A., "Carbide Precipitation in Type 304 Stainless Steel - An Electron Microscope Study," Trans. Am. Soc. Metals 43, 290 (1951).

8. Kinzel, A. B., "Chromium Carbide in Stainless Steel," J. Metals 4, 469 (1952).

9. Heger, J. J., and Hamilton, J. L., "Effect of Minor Constituents on the Intergranular Corrosion of Austenitic Stainless Steel," Corrosion 11, 6T (1955).

10. Krivobok, V. N., "Alloys of Iron and Chromium," Trans. Am. Soc. Metals 23, 1 (1935).

11. Uhlig, H. H., "Some Unexpected Properties of 18-8," Metals and Alloys 10, 66 (1939).

12. Uhlig, H. H., "The Role of Nitrogen in 18-8 Stainless Steel," Trans. Am. Soc. Metals 30, 947 (1942).

13. Uhlig, H. H., "The Comparative Effect of Carbon and Nitrogen on Intergranular Corrosion of 18/8 Stainless Steel," T. Electrochem. Soc. 87, 193 (1945).

14. Leggett, R. D., Reed, R. E., & Paxton, H. W., "Growth of Single Crystals of Stainless Steel," Trans. A.I.M.E., 215, 679, (1959).

15. Streicher, M. A., "General and Intergranular Corrosion of Austenitic Stainless Steels in Acids," J. Electrochem. Soc. 106, 161, (1959).

16. Fiore, N., B. S. Thesis, Carnegie Institute of Technology, June, 1960.

17. Basinska, Polling and Charlesby, Acta Met. 2, 513, (1954).

18. Dobrian, J., B. S. Thesis, Carnegie Institute of Technology, January, 1959.

19. Gwathmey, A. T., and Benton, A. F., "The Reaction of Gases on the Surface of a Single Crystal of Copper," J. Phys. Chem. 46, 969 (1942).

20. Young, F. W., Jr., Cathcart, J. V., and Gwathmey, A. T., "The Rate of Oxidation of Several Faces of a Single Crystal of Copper as Determined with Elliptically Polarized Light," Acta Met. 4, 145 (1956).

21. Lawless, R. R., and Gwathmey, A. T., "The Structure of Oxide Films on Different Faces of a Single Crystal of Copper," Acta Met. 4, 153 (1956).

22. Gwathmey, A. T., and Benton, A. F., "Some Experiments Showing the Directional Reactivities of Single Crystals of Copper," Trans. Electrochem. Soc., 77, 211 (1940).

23. Harris, W. W., Ball, F. L., and Gwathmey, A. T., "The Structure of Oxide Films Formed on Smooth Faces of a Single Crystal of Copper," Acta Met., 5, 574, (1957).

24. Lustman, B., "The Rate of Film Formation on Metals," Trans. Electrochem. Soc., 81, 359, (1942).

25. Lustman, B., and Mehl, R. F., "Low-temperature Oxidation of Single Crystals Trans. AM. Inst. Mining Met. Engineers, 143, 246 (1941). of Copper"

26. Mehl, R. F., McCandless, E. L., and Rhines, F. N., "Orientation of Oxide Films on Metals," Nature, 134, 1009, (1934).

27. Mehl, R. F., and McCandless, E. L., "Oxide Films on Iron," Trans. Am. Inst. Mining, Met. Engrs., 125, 531 (1937).

28. Burton, W. K., Cabrera, N., and Frank, F. C., Phil. Trans. Ray Soc. 243, A299 (1951).

29. Pound, G. M. and Hirth, J. P., J. Phys. Chem. 64, 619 (1960).

30. Frank, F. C., "Growth and Perfection and Crystals," edited by R. H. Doremus, B. W. Roberts and D. Turnbull, Wiley, New York, p. 411, (1958).

31. Hilty, D. C., Forgeng, W. D., and Folkman, R. L., Trans. AIME, 203, 253 (1955).

32. Shirley, H. T., and Truman, J. E., "Some Factors Affecting the Resistance of Austenitic Chromium-Nickel Steels to Attack by Hot Concentrated Nitric Acid," J. Iron Steel Inst. 171, 354 (1952).

33. Truman, J. E., "Factors Affecting the Testing of Stainless Steels in Boiling Concentrated Nitric Acid," J. Appl. Chem., 4, 273, (1954).

34. Huey, W. R., Trans. Am. Soc. Steel Treating 18, 1126 (1930).

35. Stickler, R., and Vinckier, A., Trans. ASM 54, 362 (1962).

36. Rhodin, T. N., Corrosion 12, 123t, (1956).

37. DeLong, W. B., ASTM, Special Technical Publication 93, 211, (1949).

38. Nielsen, N. A., Werkstoffe und Korrosion 10, 429, (1959).

39. Rosenberg, S. J., and Irish, C. R., J. Research Nat. Bur. Stand. 48, 40, (1952).

Fig. 1 Typical appearance of a melt-grown single crystal of 20Cr 20 Ni austenitic stainless steel after 123 hours exposure to pure boiling nitric acid. (x50)

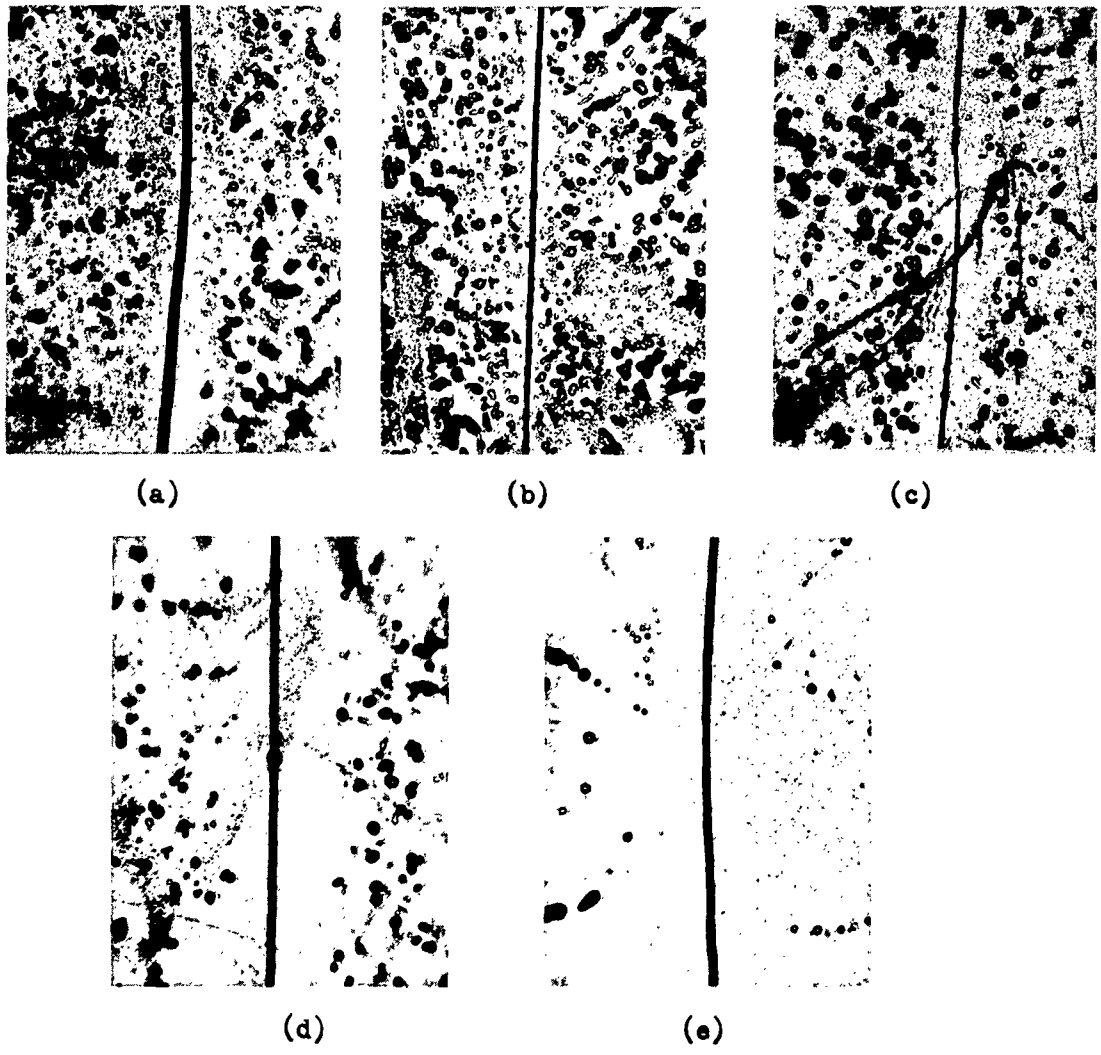


Fig. 3 (x500) The influence of annealing temperature on the morphology of grain boundary attack. All specimens were water quenched after the following heat treatments. (a) 650°C for 18 hours, (b) 800°C for 19 hours, (c) 900°C for 12 hours, (d) 1000°C for 16 hours, (e) 1100°C for 19 hours.

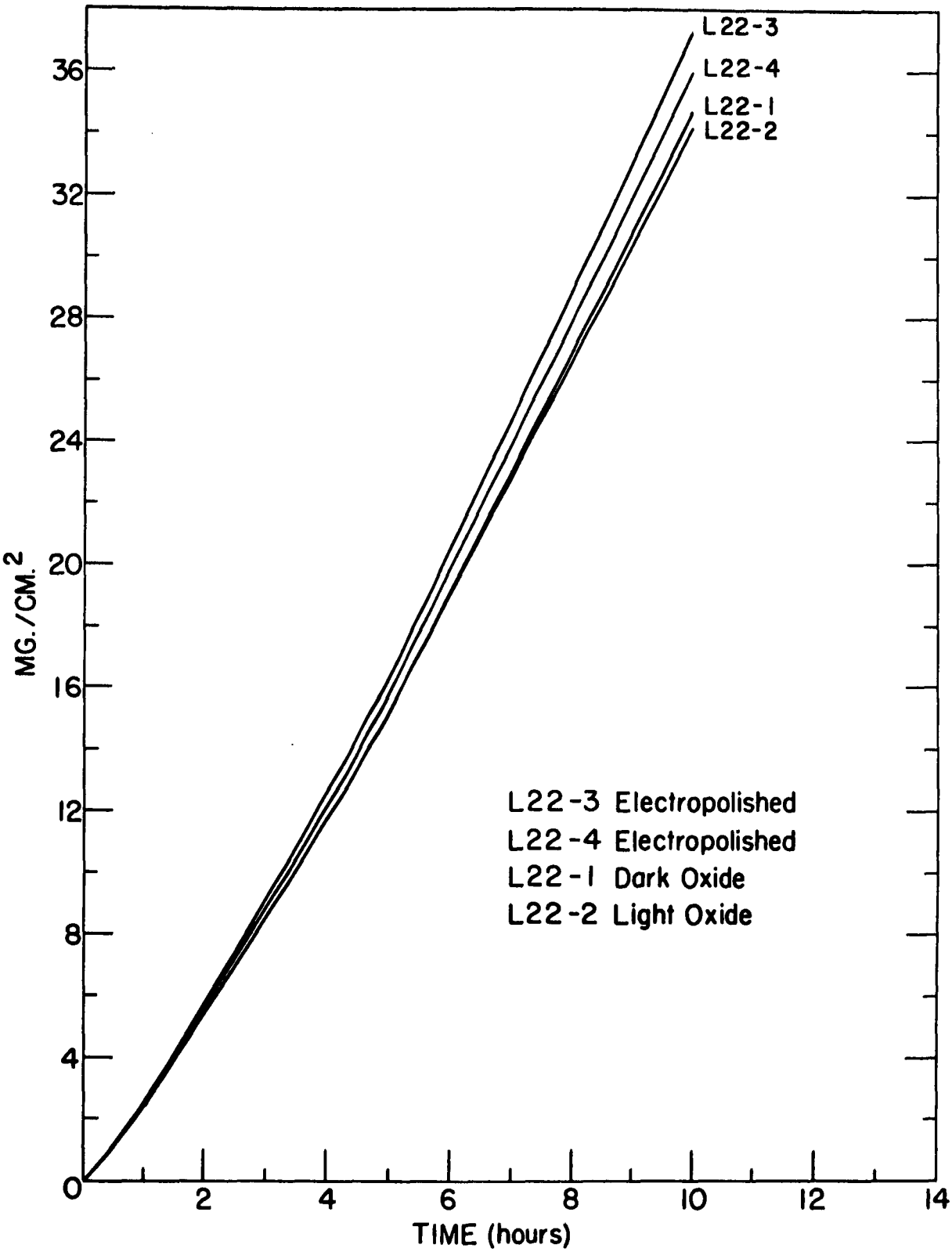


Fig. 2 Corrosion rate (weight loss) as a function of time in various samples cut from crystal L22. Prior to corrosion testing, L22-1 was oxidized in air to give a noticeable dark oxide film, L22-2 had a pale straw oxide, and L22-3 and L22-4 were electropolished in the standard fashion described in the text.

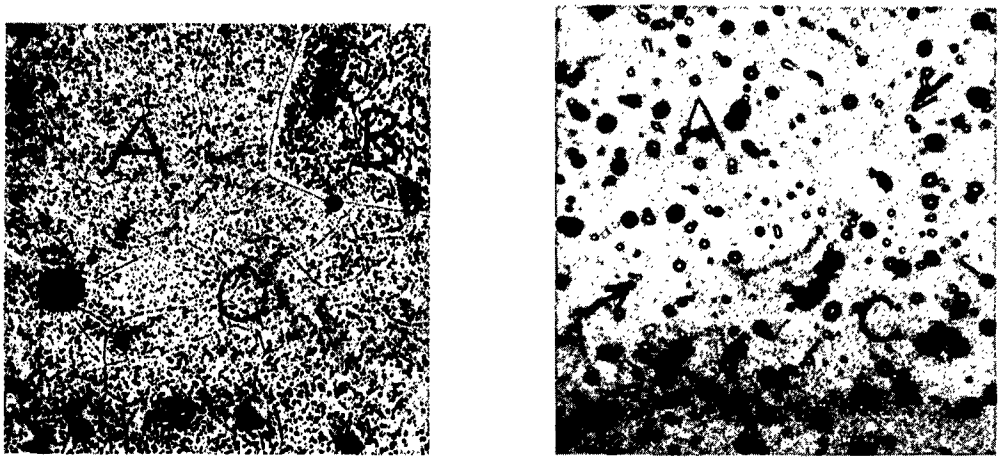


(a) (b)

**Fig. 4** Relative grain boundary attack as a function of misorientation between grains. The boundary and pit free zone between A and B, and B and C is clear; that between A and C is hardly visible. Grains A and C have a common (100) plane with a 10° angle between the <100> directions in this plane in each grain. A and B, and B and C have no good matching. (a) 100x (b) 500x

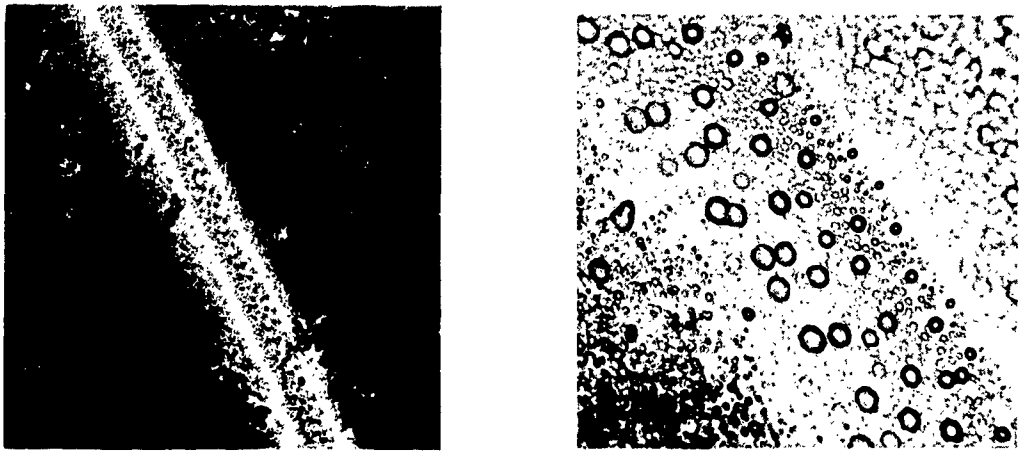

(a) (b)

**Fig. 6** Corrosion in 20% Cr 20% Ni specimen of a grain boundary whose pole is 15° from the surface normal. Corroded 4 hours in boiling impure nitric acid. (a) 100x (b) 500x

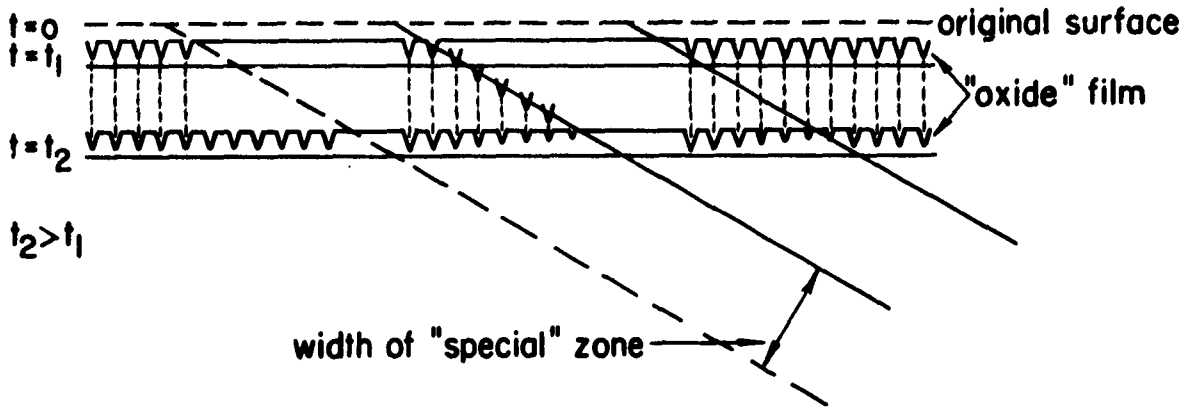


Fig. 5 Schematic illustration of attack at oblique grain boundary showing development of pits all over surface by suitable nucleation and subsequent growth.

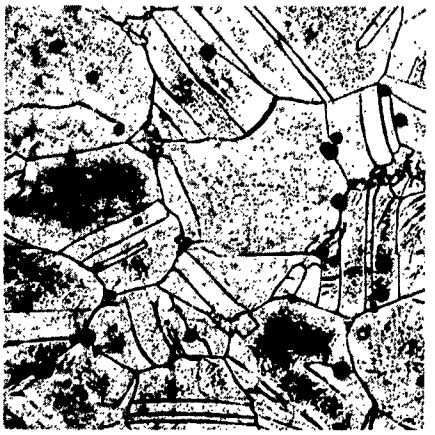

(a)

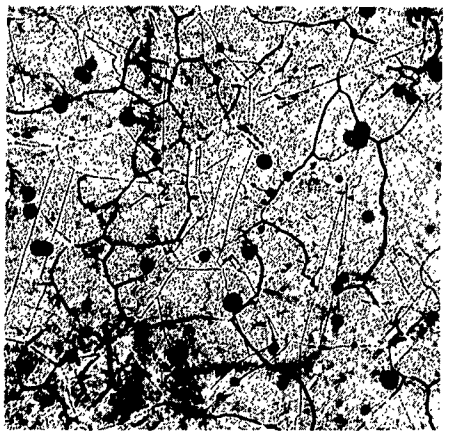

(b)

(c)

Fig. 7 Corrosion appearance of original polycrystalline material. (a) as hot forged, (b) annealed at 900°C for 24 hours and water quenched, (c) annealed at 1100°C for 24 hours and water quenched. (All 100x)

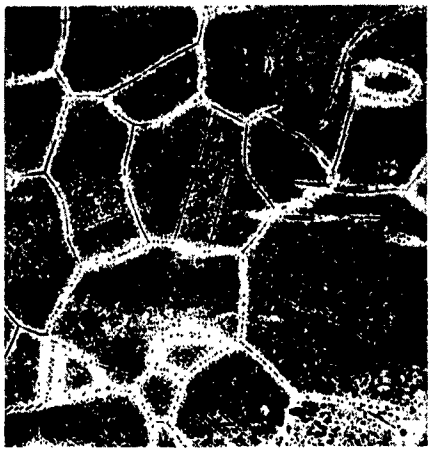

Fig. 8 Corrosion appearance of a crystal cold-rolled 65%, recrystallized at 1100°C for 24 hours, cooled to room temperature, annealed at 900°C for 24 hours and water quenched. Grain dropping was not observed with this sample, and the corrosion rate was constant. (100x)

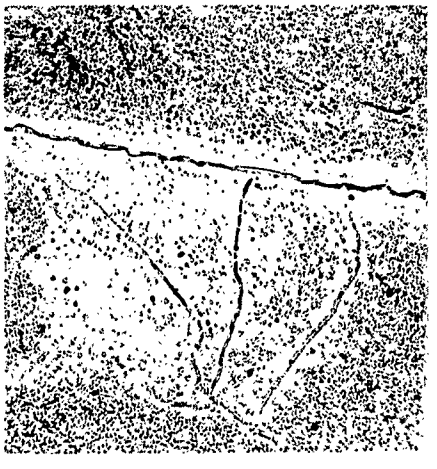

Fig. 10 Ingot L-20 (0.24%N) after quenching from 800°C and corroding for 1 hour in impure acid. Note pronounced boundary precipitation. (500x)

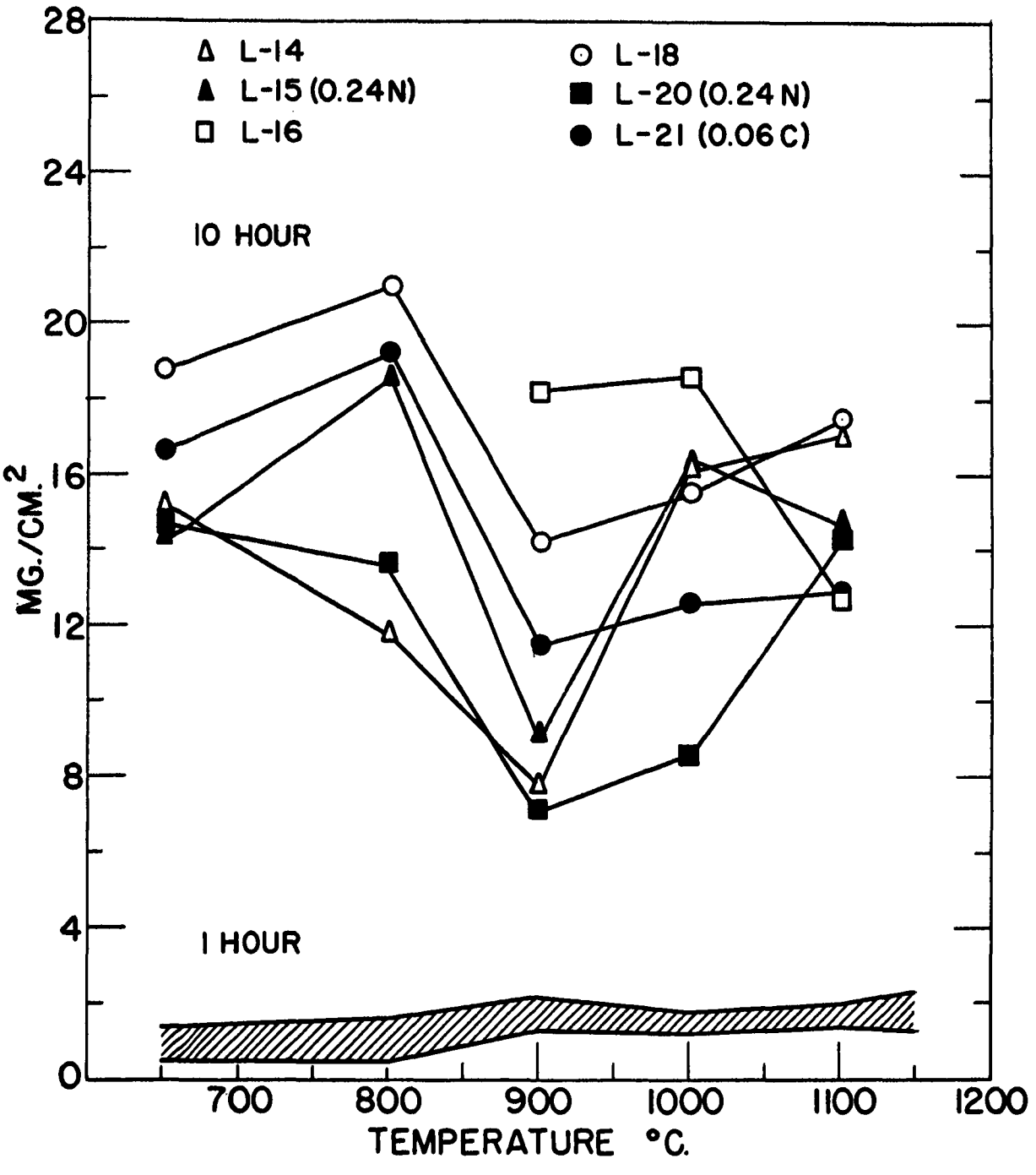


Fig. 9 Comparison of the rate of attack of high carbon and nitrogen samples with those of various high purity samples.